

# The Squall Line of 21 July 1992 in Southern Germany: An Observational Case Study

S. P. HAASE-STRAUB<sup>1,3</sup>, M. HAGEN<sup>2</sup>, T. HAUF<sup>2</sup>, D. HEIMANN<sup>2</sup>, M. PERISTERI<sup>1</sup>, R. K. SMITH<sup>1</sup>

<sup>1</sup> Meteorologisches Institut der Universität München, Theresienstraße 37, 80333 München, Germany

<sup>2</sup> Deutsche Forschungsanstalt für Luft- und Raumfahrt (DLR), Institut für Physik der Atmosphäre, Oberpfaffenhofen, 82234 Weßling, Germany

<sup>3</sup> Present address: Bayerische Rückversicherung AG, Sederangerstraße 4-6, 80538 München, Germany

(Manuscript received March 25, 1996; accepted April 15, 1997)

## Abstract

On 21 July 1992 a fast moving squall line developed over southwestern Germany and Switzerland in the prefrontal area of a cold front. It moved eastwards and merged with a stationary convergence line ahead of it. The merger occurred in a region where a mesoscale network of 14 automatic weather stations was in operation and it was well documented by the polarimetric Doppler radar at Oberpfaffenhofen near München. In this paper we describe the characteristics of the squall line and its environment based on analyses of the radar and surface data, and on serial radiosonde soundings. The meso- $\gamma$ -scale features are also described including the gust-front formation and evolution.

## Zusammenfassung

### Die Squall Line vom 21. Juli 1992 in Süddeutschland: Eine Fallstudie

Am 21. Juli 1992 entwickelte sich vor einer von Westen heranziehenden Kaltfront über Südwestdeutschland und der Schweiz eine 'Squall Line'. Diese zog sehr rasch nach Osten und vereinigte sich mit einer vor ihr befindlichen, stationären Konvergenzlinie. Der Zusammenschluß trat in einem Gebiet auf, in dem zu dieser Zeit ein mesoskaliges Meßnetz mit 14 automatischen Stationen in Betrieb war. Zudem wurde er von dem polarimetrischen Doppler-Radar in Oberpfaffenhofen nahe München erfaßt. In dieser Arbeit beschreiben wir die Charakteristiken dieser Squall Line und ihrer Umgebungsbedingungen. Die Analysen basieren auf Radar- und Bodendaten, sowie auf einer Reihe von Radiosondenaufstiegen. Es werden die meso- $\gamma$ -skaligen Strukturen, einschließlich der Entstehung und Entwicklung einer Böenlinie, dargestellt.

## 1 Introduction

Research into midlatitude thunderstorms has been most vigorous in the United States where severe thunderstorms, frequently accompanied by large hail and sometimes tornadoes are relatively common. A long term observational research programme into these storms has been in progress for many years in Oklahoma, the state with the largest frequency of severe hailstorms and tornadic thunderstorms (Court and Griffiths, 1985). Recently, Houze et al. (1990) presented a climatological study of springtime storms in Oklahoma and sought to classify the common types of mesoscale organization of storms

accompanied by heavy precipitation. They found from radar observations that in two-thirds of the cases, the convection was organized in a line which preceded an extended stratiform precipitation area. Prior to this, Bluestein and Jain (1985) carried out a similar study of squall lines in the Oklahoma region in springtime and identified four basic types of development. In another climatological study, Wyss and Emanuel (1988) investigated the prestorm environment of midlatitude prefrontal squall lines, based on a data set of 60 cases from all seasons and from various geographical regions of the continental United States. This research, as well as numerous observational case studies during the last two decades (see

e.g. Houze and Hobbs (1982), Kessler (1985), Houze (1993), Emanuel (1994, Chapter 9 and refs.) has gone hand-in-hand with significant progress in our theoretical understanding of storm structure and evolution, based largely on numerical modelling studies (see e.g. Emanuel, 1994, Chapter 11 and refs.).

In general, severe thunderstorms over Europe are less frequent and more benign than their counterparts over the midwest of the United States and rarely do they spawn major tornadoes. Nevertheless, storms occasionally reach an intensity sufficient to produce large hail (golf-ball size and over), severe wind gusts, and to cause a swath destruction with major damage to property and crops, injuries to persons and occasionally some fatalities.

Research into severe thunderstorms over Europe is not without its history with some notable case studies including the Wokingham Storm in 1959 (Browning and Ludlam, 1962), the Hampstead Storm in 1975 (Keers and Westcott, 1976, Miller, 1978), and the München Hailstorm in 1984 (Heimann and Kurz, 1985; Höller and Reinhardt, 1986; Brugge and Moncrieff, 1992). In recent years there has been a particularly active research programme in Switzerland, where summertime hailstorms are common. Climatological studies there are reported by Schiesser et al. (1995) and Huntriesser (1995).

A climatological study of organized convective storms there, within the range of the Oberpfaffenhofen<sup>1</sup> polarimetric Doppler radar, has been carried out by Höller (1994). Within the 6-years period 1987–1992, Höller reported 207 thunderstorm days and found line-oriented storms on 93 of these (45 % of the total). Of the latter, 18 were classified as squall-line days, i.e., days on which a squall line developed within the range of the Oberpfaffenhofen radar. The kinematics of and precipitation formation in a squall line that formed ahead of a southeastward moving cold front over southern Germany were investigated by Meischner et al. (1991) using polarimetric Doppler radar measurements. However, neither the mesoscale development of the squall line, nor its synoptic environment were documented in detail.

Statistics for storm development in Upper Bavaria point to the Allgäu to be a preferred region for thunderstorms. Here, 35 days with thunderstorms compare with a mean value of 28 thunderstorm days in the Alpine forelands (Pelz, 1984). The reason for the Allgäu to be favourable to thunderstorm development is thought to lie in the particular orography and

its orientation relative to the large-scale southwesterly flow.

In the summer of 1992 a field experiment named CLEOPATRA was carried out in southern Germany to study the hydrological cycle on a regional scale. (Meischner et al., 1993). One component of the experiment was the “mission squall line”, at the forefront of which was the hypothesis that severe thunderstorms develop in southwesterly air streams in early spring and summer, when (i) the low-level moisture advection is large to the north of the Alps, and (ii) the cross-mountain airflow induces low pressure on the northern side of the Alps leading to low-level convergence over Switzerland and southern Germany. It was hypothesized also that these conditions lead to patterns of vertical wind shear and wind turning with height that are conducive to the formation of severe storms. The present paper analyzes a squall line that occurred on 21 July 1992 during the CLEOPATRA experiment. The comprehensive data set for this event is documented by Haase-Straub et al. (1994) and Finke and Hauf (1997) on a CD-ROM.

The squall line was one of a series of severe storms that crossed central Europe on that day. These storms were part of a frontal system that extended from a low pressure centre over the North Sea to Spain. Some slightly clustered storms developed over southern France already in the morning on 21 July and moved in north-westerly direction. Ahead of these storms in a 500 km wide north-south running belt isolated and nearly stationary storms formed. When over Switzerland the former storms merged with the stationary ones a well expressed squall line developed. This squall line moved eastwards and crossed the special CLEOPATRA observation network in southern Germany. During the period from 1600 UTC to 2000 UTC on 21 July, the squall line approached and merged again with an almost stationary convective line that had formed shortly before 1800 UTC, just to the east of Lake of Constance.

This paper describes the regional aspects of this squall line based on the data obtained from this network. The synoptic environment in which the squall line developed is discussed in Section 2. The observational data set available for the study is described in Section 3. In Section 4 we describe features of the meso- $\beta$ -scale (20 to 200 km) organization, while in Section 5 we consider aspects of the meso- $\gamma$ -scale (2 to 20 km) structure of the squall line. A summary and conclusions are presented in Section 6.

<sup>1</sup> Oberpfaffenhofen lies approximately 25 km west-southwest of München.

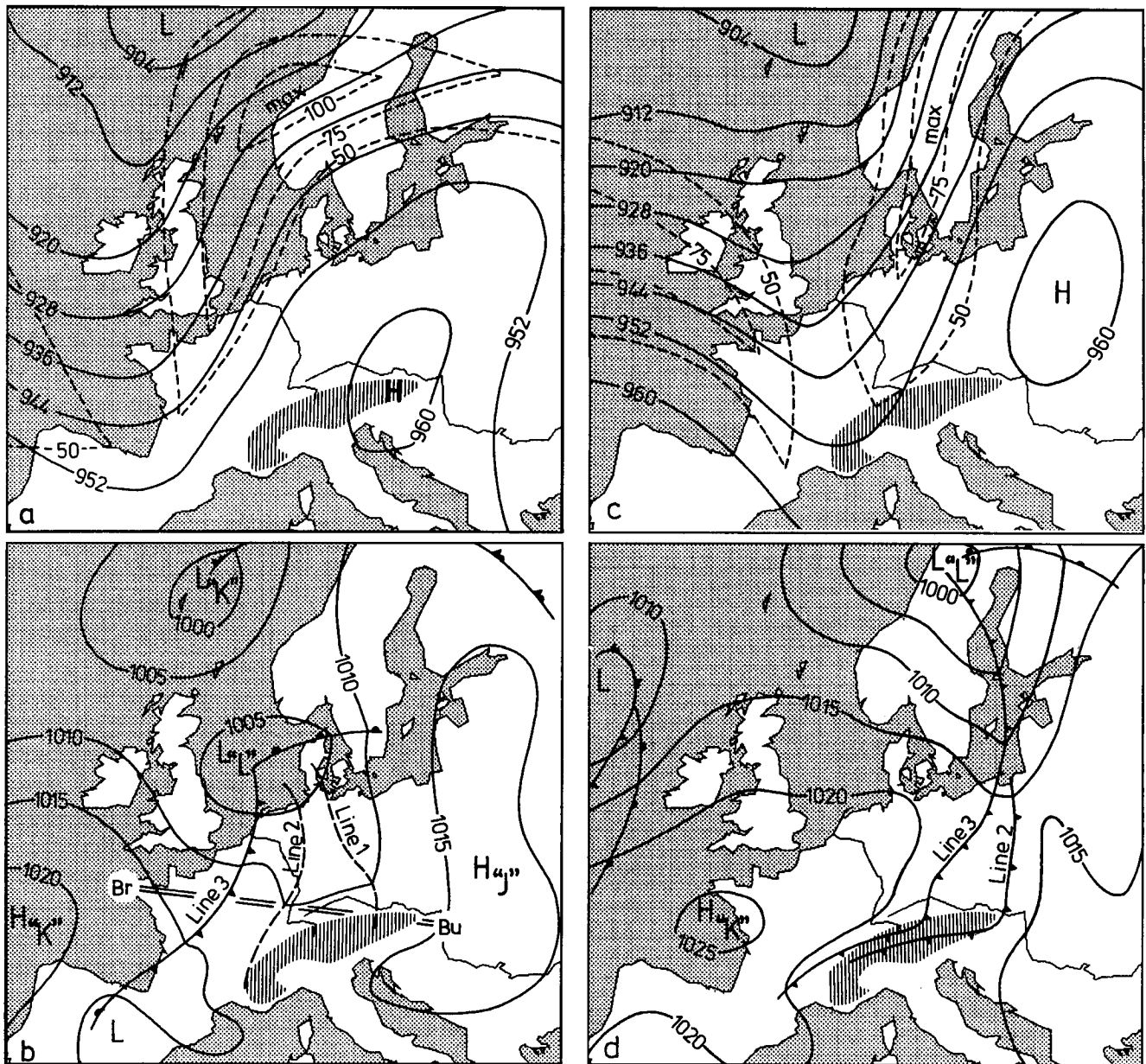


**Figure 1:** 300 hPa geopotential and windspeed analyses (a,c) and mean sea level isobaric chart (b,d) of 21 July 1992, 1200 UTC (a,b) and 22 July 1992, 1200 UTC (c,d), adapted from the European Meteorological Bulletin issued by the Deutscher Wetterdienst and the Berliner Wetterkarte issued by the Institut für Meteorologie of Freie Universität Berlin. The hatched area indicates the Alps. The dashed lines in (a,c) represent the 50, 75, and 100 kt isotachs. The surface charts (b,d) show the position of Lines 1, 2, and 3 (see text). The double line from Br to Bu in (b) shows the basis for Figure 3.

## 2 Synoptic Development

This section describes the synoptic-scale environment in which the squall line of 21 July 1992 was embedded. The main attention is focussed on horizontal and vertical cross-sections of thermodynamical fields obtained from conventional surface and upper-air data.

The situation at 1200 UTC on 21 July is shown in Figure 1. In the upper air, at 300 hPa (Figure 1a), a strong southwesterly to south-southwesterly air flow extended from France across the North Sea to Norway with the wind speed reaching  $40 \text{ m s}^{-1}$  (80 kn) above Paris. By this time, the surface low "K" had moved to the area between Iceland and Norway (Figure 1b). The cold front originating from low "L"

trailed southwestwards to northern Spain. It separated a cool maritime polar air mass (mP) that was advancing from the Atlantic Ocean from a warm subtropical maritime air mass (mS) to the east. East of the Rhine the subtropical maritime air had acquired the character of a hot continental air mass (cS) under the influence of the surface high pressure system (designated "J") over central and eastern Europe.

We discuss now the surface weather analysis for 1200 UTC of 21 July 1992 in detail as this was 6 to 12 hours prior to the appearance of severe storms over Switzerland and southern Germany. A comparison of published weather maps, viz. the "European Meteorological Bulletin" issued by the Deutscher Wetterdienst and the "Berliner Wetterkarte" issued by the Freie Universität Berlin, pointed to the existence of three change lines in both wind and pressure south of low "L". However, each of the maps shows only two of the change lines, but not always the same two! In Figure 1b all three lines are drawn and they are defined as follows:

#### Line 1:

This line was analyzed solely in the Berliner Wetterkarte where it was classified as a "convergence line". It extended from the centre of low "L" to Denmark and from there to Upper Austria, terminating at the northern edge of the Alps. The line was embedded in a marked trough of low pressure and separated easterly to southeasterly winds on its eastern side from southwesterly winds on its western side. There was no significant temperature contrast across this line, nor was any significant weather activity observed along it.

#### Line 2:

The second line was analyzed in both weather charts. It was classified as a convergence line in the European Meteorological Bulletin, but as a cold front in the Berliner Wetterkarte. As in the case of Line 1 it originated near the centre of the Low "L", but took a course west of Line 1 over the German Bight, western Germany and eastern France. The northernmost and southernmost sections of the line, north of 50°N and south of 48°N, were situated also in a well marked surface-pressure trough, with the wind turning from south or southwest to west or northwest. Generally, the wind speed was stronger on the western side of the line, particularly in the northernmost section. The temperature was typically a few degrees lower west of the line, ranging between 26 to 29°C, compared with values between 29 and 33°C to the east of it. Showers and thunderstorms were observed along the line over northern Germany.

#### Line 3:

The third line was analysed only in the European Meteorological Bulletin where it was classified as a cold front. It extended from the North Sea over The Netherlands, Belgium and central France to the Bay of Biscay and northern Spain. The line was characterized by a weak pressure change along much of its length. Its existence is corroborated by a marked wind shift from southwest to northwest across the relevant section of the line. In general, the surface temperatures were lower on the western side of the line with values ranging between 18 and 22°C. Occasional rain was observed along the line.

We suggest that the three lines were real features and constituted the frontal transition zone of the low-pressure system "L". In summary they are classified as follows:

- Line 1: a convergence line within the continental subtropical air mass (cS).
- Line 2: a convergence line or (weak) cold front separating the continental air mass (cS) from the maritime air mass (mS) that flowed in from the southwest.
- Line 3: a cold front associated with a well marked air-mass change from maritime subtropical air (mS) to maritime polar air (mP).

Similar frontal transition zones have been observed in association with summertime cold fronts over southeastern Australia (Garrett et al., 1985).

The vertical structure of the frontal transition zone at 1200 UTC on 21 July 1992 is indicated by cross-sections of potential temperature  $\theta$ , and equivalent-potential temperature<sup>2</sup>  $\theta_e$ . These were constructed from radiosonde data at stations across central Europe, namely, from west to east: Brest, Trappes (near Paris), Nancy, Stuttgart, München, Wien, and Budapest.

The potential temperature cross-section (Figure 2a) shows that the warmest upper-air temperatures were above Wien, i.e. near Line 1. In the lower atmosphere the maximum potential temperatures occurred between Stuttgart and Nancy, i.e., just to the east of Line 2. Between these stations the cross-section shows a slight decrease of potential temperature towards the west and a more rapid fall associated with Line 3 between Nancy and Trappes.

<sup>2</sup> Throughout this paper we have calculated the pseudo-equivalent potential temperature.

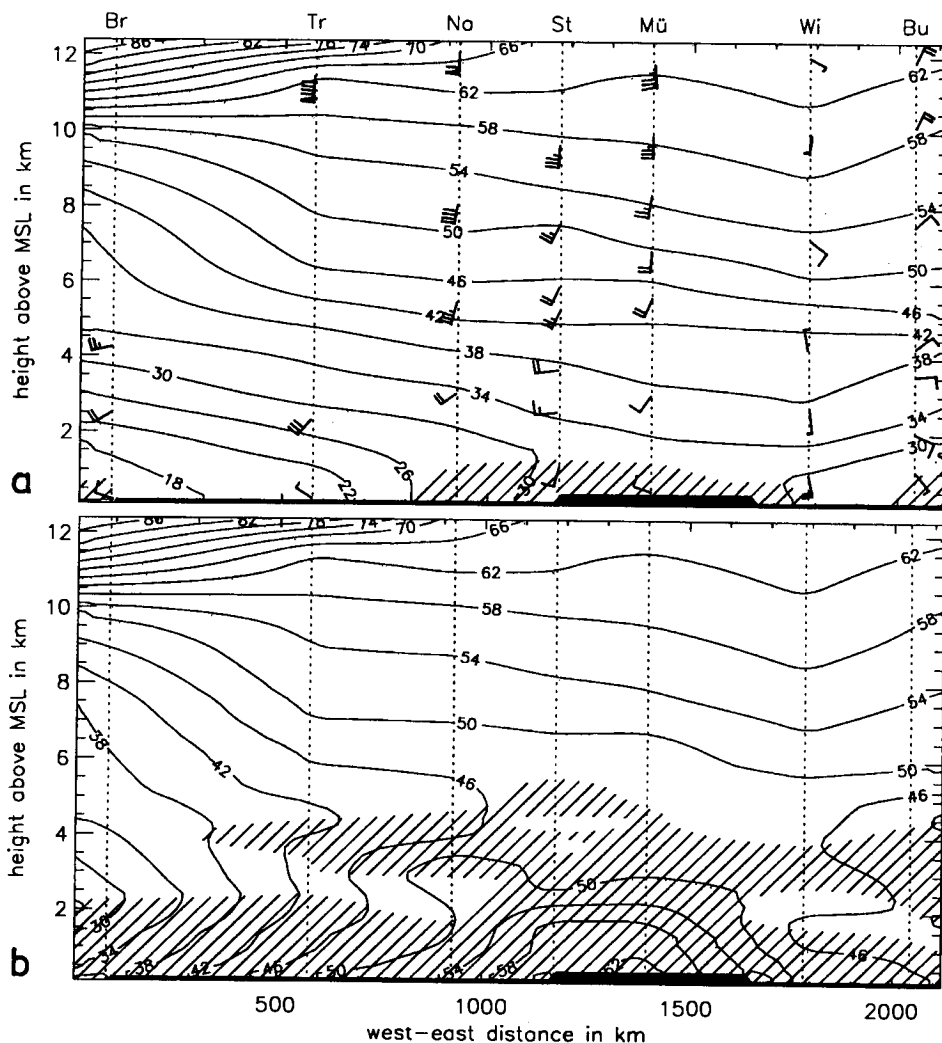


**Figure 2:** Vertical west-east cross-sections (from Brest, France to Budapest, Hungary; the baseline is shown in Figure 1b) of potential temperature  $\theta$  in  $^{\circ}\text{C}$  (a), and equivalent-potential temperature  $\theta_e$  in  $^{\circ}\text{C}$  (b), based on the radiosonde soundings on 21 July 1992, 12 UTC. Winds in (a) are given in conventional notation (knot). Hatched areas in (b) indicate negative vertical gradients of  $\theta_e$ .

The equivalent-potential temperature cross-section (Figure 2b) indicates especially high values, more than  $60^{\circ}\text{C}$ , between München and Stuttgart. This area had also the highest potential instability as characterized by the decline of  $\theta_e$  through the lowest 5 km. Only in the maritime polar air mass on the western side of Line 3 was significant potential instability no longer present. Above Brest this air mass had already attained a thickness of 8 km. The maritime polar air was characterized by equivalent-potential temperatures below  $40^{\circ}\text{C}$ .

Figure 3 shows the values of the convective available potential energy (CAPE) at 1200 UTC at all radiosonde stations across central Europe and isolines of this quantity. The CAPE is defined as the verti-

cal integral of the buoyancy force per unit mass of a pseudo-adiabatically lifted air parcel from a certain level  $z_L$  near the ground to the level of neutral buoyancy, i.e. to the highest level at which the buoyancy force vanishes. In our case CAPE was calculated for starting levels between  $z_L = 0$  and  $z_L = 500$  m in steps of 100 m and subsequently averaged. Along Line 2 the CAPE significantly exceeded  $1000 \text{ J kg}^{-1}$  and clearly indicates the high potential for deep convection in this area.

On the following day, at 1200 UTC on 22 July, the axis of the eastern Atlantic upper-air trough had moved to a position roughly defined by the mouth of the Rhine and the mouth of the Rhone while the surface low "L" had moved along the Norwegian coast

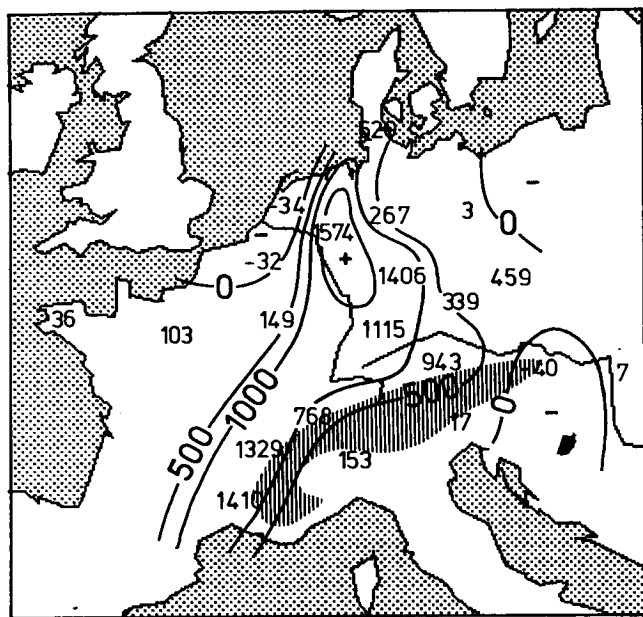


**Figure 3:** Average values of CAPE (in  $\text{J kg}^{-1}$ ) on 21 July 1992, 12 UTC, at radiosonde stations across central Europe. The average CAPE is for air parcels lifted pseudo-adiabatically from heights 0 m, 200 m, 300 m and 400 m above the surface.

towards the north (Figures 1c,d). The frontal zone of this low extended over the Baltic Sea, across western Poland and Bohemia to the Alps. On its western side a new high pressure zone (designated "K") had formed, extending from the eastern Atlantic Ocean to western Europe.

The surface weather map of the European Meteorological Bulletin at 1200 UTC on 22 July indicated only one line, viz. Line 3. As before it was classified as cold front although it had become retrograde in its southernmost part. The Berliner Wetterkarte continued to analyze Line 2 as a cold front which had crossed northern Austria and was entering Slovakia, Hungary and southeastern Austria. In contrast to the previous day, Line 3 was analyzed also in the Berliner Wetterkarte and, consistent with the European Meteorological Bulletin, was classified as cold front. This line was analyzed in the same position in both maps. The existence of Line 1 at this time was no longer indicated by the data available. Figure 1d shows the corresponding positions of Line 2 and Line 3 at 1200 UTC on 22 July 1992.

The severe storms, which developed during the passage of the frontal zone in western and northern Switzerland and southern Germany, were apparently caused by a combination of synoptic-scale circumstances. Thermodynamic aspects of these are

1. the large temperature contrast across the frontal zone,

2. the coincidence of high temperatures and high moisture content in the air mass ahead of Line 2, as indicated by comparatively high values of the equivalent-potential temperature,
3. the strong potential instability within the frontal zone, in particular between Line 1 and Line 2,
4. high values of CAPE along Line 2.

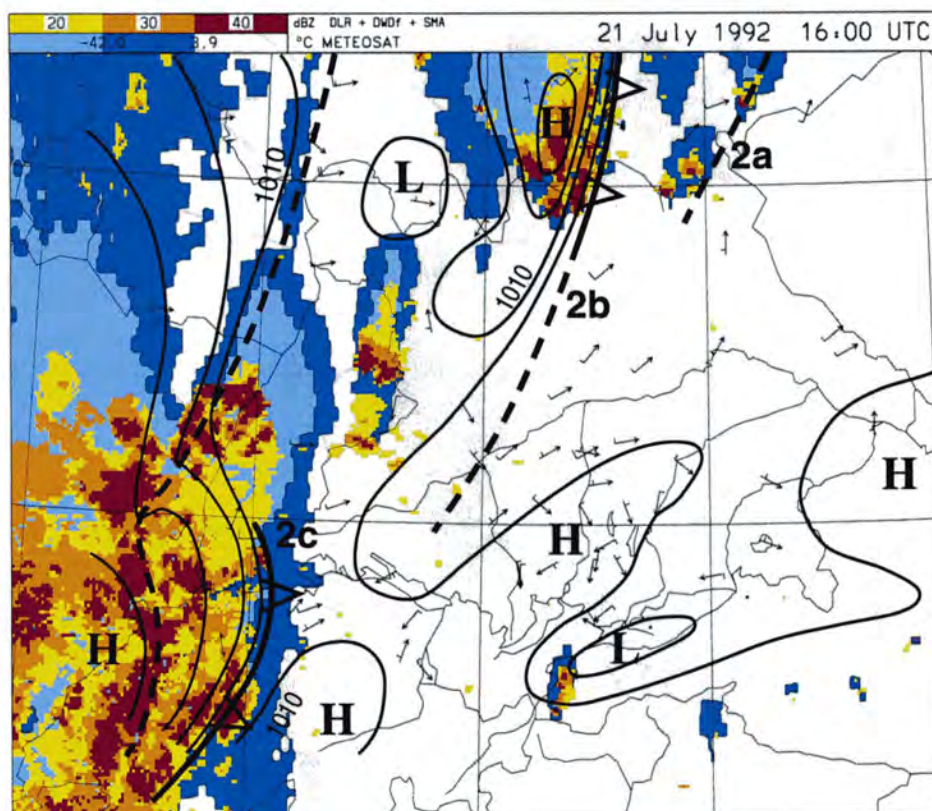
We hypothesize that mesoscale lifting released the potential instability. This is in agreement with the numerical simulations of Prenosil et al. (1995) on the same case. Although the dynamical aspects of the squall line development could not be determined quantitatively on the basis of the available upper-air observations. It is well known that the inflow regime on the eastern side of the jet stream above a frontal zone is generally favorable for large-scale ascent. In combination with the potential instability, the lifting probably caused the release of static instability and gave rise to deep convection. It would have been likely that additional instability resulted from the cold-air advection in the middle troposphere, which was indicated by the vertical wind shift within the air mass ahead of Line 2.

### 3 Observational Network

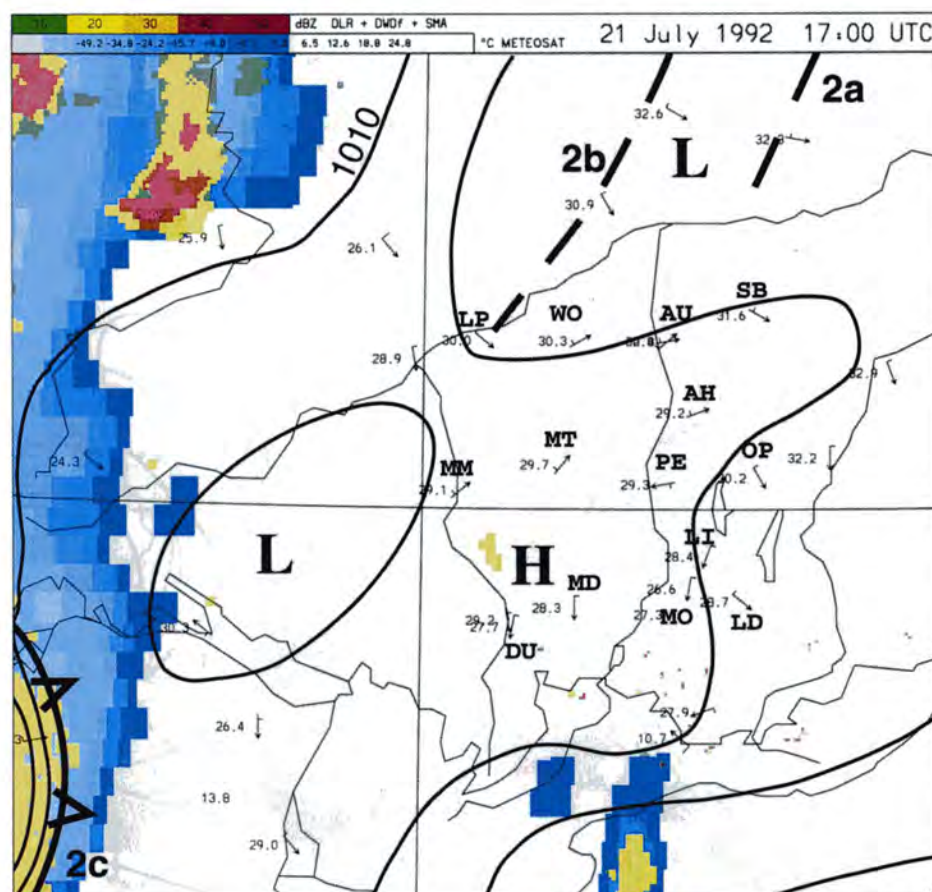
Measurements made during the CLEOPATRA experiment included (see also Finke and Hauf, 1997):

- three-dimensional scans with the DLR-polarimetric Doppler radar (POLDIRAD) in Oberpfaffenhofen (Schroth et al., 1988);
- serial radiosonde soundings at Penzing, 27 km west of Oberpfaffenhofen;
- data from a mesoscale network (mesonet) of surface stations in a region southwest of München;
- data from an instrumented meteorological tower in Garching, located about 20 km north of München and 50 km northeast of the north-eastern edge of the mesonet (Lösslein, 1994);
- a Doppler sodar and a high frequency microbarograph array located in Lichtenau, 27 km southwest of Oberpfaffenhofen. These experimental data were combined with routine data and used to construct a detailed mesoscale analysis of the squall line of 21 July 1992 over southern Germany.



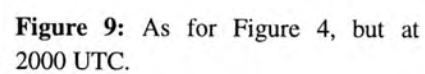
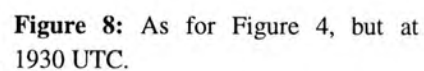


**Figure 4:** Composite of 21 July 1992 at 1600 UTC, of METEOSAT infrared images, of radar reflectivity observed by the DLR, DWD at Frankfurt and the SMA radar-network. Overlaid are the surface pressure analysis and the observations of surface winds by the national weather services and the mesonet.



**Figure 5:** As for Figure 4, but at 1700 UTC.







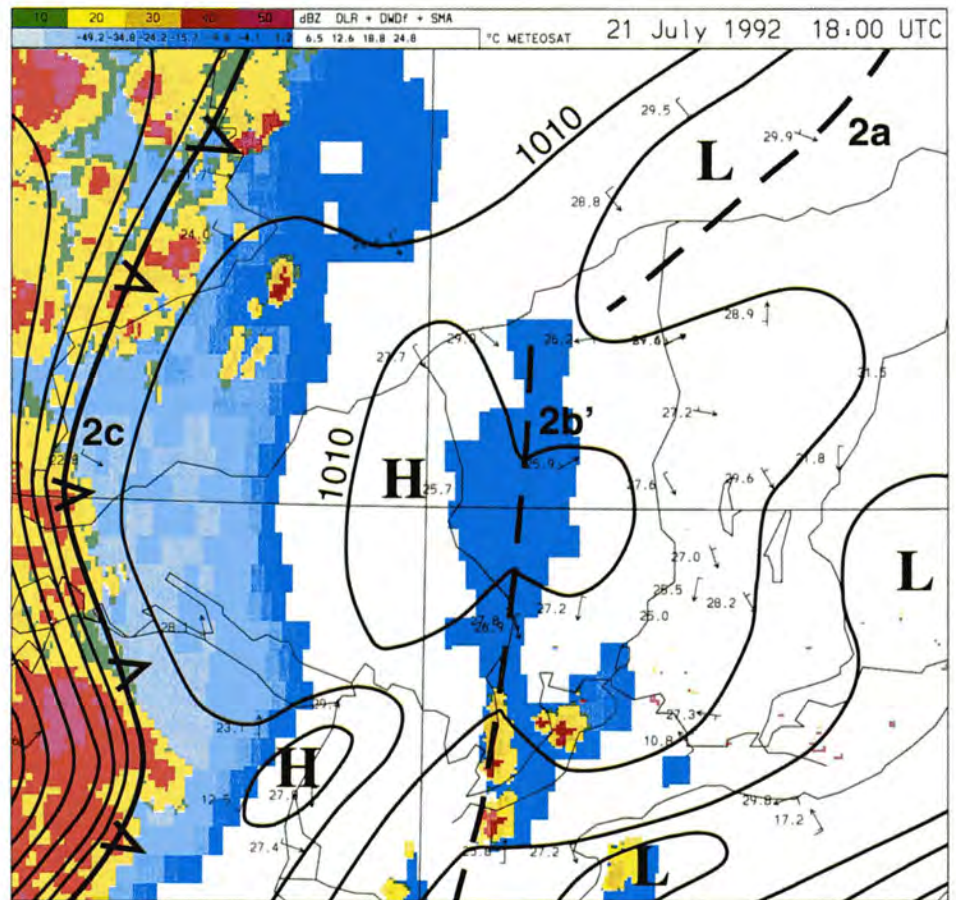


**Figure 6:** As for Figure 4, but at 1800 UTC.

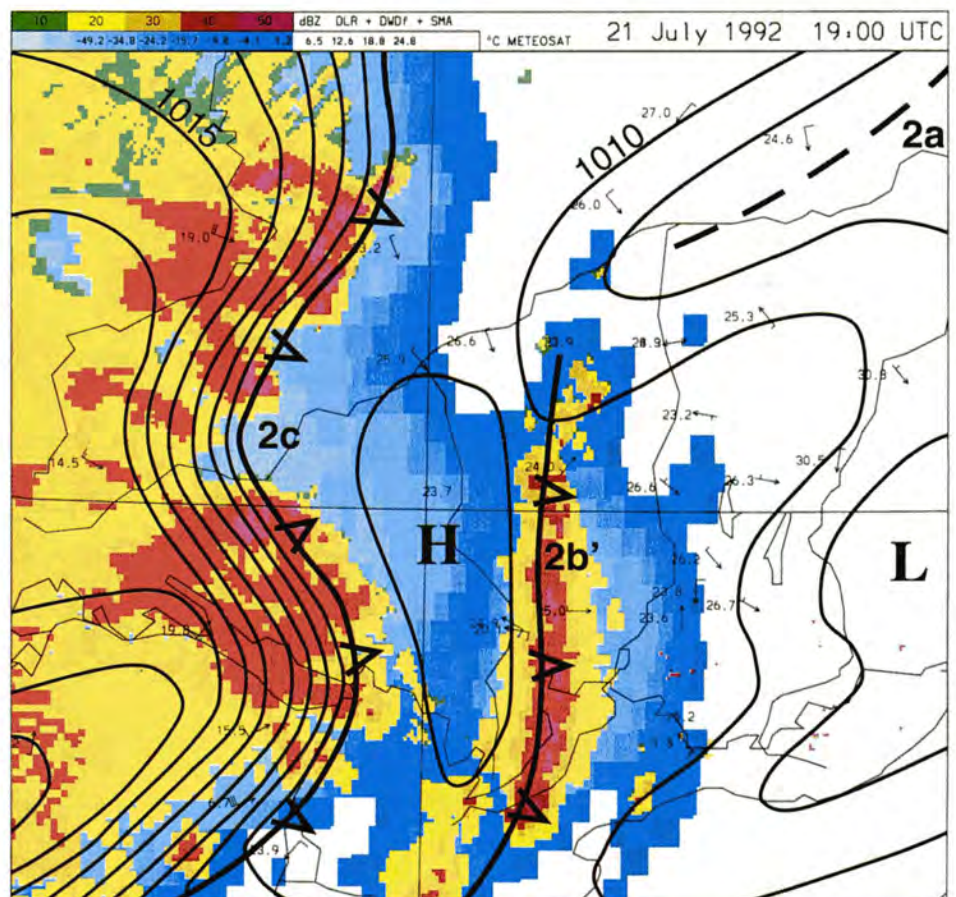


**Figure 7:** As for Figure 4, but at 1900 UTC.

The polarimetric capability of the Doppler radar enables insights into precipitation and hail formation processes to be obtained (Hagen and Höller, 1994). Sequences of PPI<sup>3</sup> scans at elevation angle of 0.8° were used to analyze the structure of the precipitation field associated with the squall line.

The radiosonde soundings at Penzing were carried out using a Väisälä MARWIN-sonde system in which wind speeds are obtained using the Omega navigation system (Väisälä MET Technical Manual, Technical Description, July 1989). On 21 July 1992 four soundings were carried out at the following times: 1000 UTC, 1400 UTC, 1800 UTC, and 2100 UTC. The first three soundings were made before the passage of the squall line, the last one just after its passage.

The surface mesonet consisted of 14 automatic weather stations which were deployed in a region of about 100 × 100 km<sup>2</sup> within range of the Doppler radar. Each station measured pressure, air temperature (both dry- and wet-bulb), and wind speed and direction, with a time resolution of 2 minutes. All meteorological parameters except pressure were measured at a height of about 3 m above ground level. The pressure was measured at ground level to minimize the stagnation pressure fluctuations caused by the wind. The station pressure was reduced to the height of the DLR station (581 m above mean sea level).

The Doppler sodar was installed to observe the boundary-layer structure (Beyrich et al., 1994) and the microbarograph array was established to investigate gravity-wave disturbances (Finke and Hauf, 1994).

#### 4 Meso-β-Scale Observations

The meso-scale evolution of the various lines between 1200 and 2400 UTC on 21 July 1992 as observed by radar and satellite over Germany and the northern Alpine region was shown by Hagen and Heimann (1994). In this paper we concentrate on the development in the northern Alpine foreland.

At 1600 UTC the situation over the northern Alpine forelands was dominated by Line 2, which formed the leading edge of a vigorous west to southwesterly airstream as it moved eastwards (Figure 4). Closer analysis indicates that, in fact, this line was composed of several separate convergence Lines 2a, 2b and 2c. The German radar composite (Hagen and

Heimann, 1994) shows parallel lines of convective activity along Lines 2a, 2b and 2c mainly across northern Germany. At this time the major precipitation area behind the Line 2c, was still located over central Switzerland. Note the region of low pressure on the northern side of the Alps ahead of Line 2. Typically, such lows are orographically induced when there is a southwesterly airstream across the Alps.

A composite analysis of the situation at 1700 UTC is shown in Figure 5. In the northern Alpine forelands, Lines 2a and 2b were embedded in an area of weak pressure gradient, whereas the westernmost line (Line 2c) was located to the southwest (near the edge of the figure). During its passage across Switzerland, Line 2c had already caused considerable hail damage.

Between 1800 UTC and 1900 UTC a new convergence line formed at the northern edge of the Alps and within one hour had extended northwards about 100 km while moving eastwards at 5 m s<sup>-1</sup>. Time series of various variables at the mesonet sites for the time period from 1600 UTC to 2300 UTC are shown in Figure 10. The time series show that the development of the new line was accompanied by an increase of the equivalent-potential temperature,  $\theta_e$ , at the mesonet stations Leipheim (LP) and Memmingen (MM), indicating the advection of relatively warm moist air by the southwesterly near-surface flow around the western edge of the Alps. This air replaced drier air that had been convectively heated to a depth of some 2 km. Note that the station Dürach (DU) did not show an increase  $\theta_e$ , possibly because it was sheltered by the local topography. At about 1800 UTC (see Figure 6) a single north-south oriented line (Line 2b') formed over the Allgäu region of southern Germany. This line (the Allgäu line) extended as far north as the river Danube and according to satellite imagery had cloud tops around 0°C, corresponding to a height of about 4 km above the surface (see the infrared-temperatures in Figure 6). Thunderstorms were observed at the southern end of the line in the vicinity of the Alps. The relationship between the new convergence Line 2b' with Lines 2a and 2b further north (Figure 4) is not clear. Objective analyses of the mesonet data for the time period from 1812 UTC to 1854 UTC show the presence of the low-pressure area just north-northeast of the Allgäu line (see Luckner and Smith, 1994). The surface winds during this period were light, but indicated weak convergence at the northern end of the Allgäu line. The Allgäu line (2b') remained approximately stationary until about 1930 UTC when it was overrun by the squall line (2c).

<sup>3</sup> Plan Position Indicator

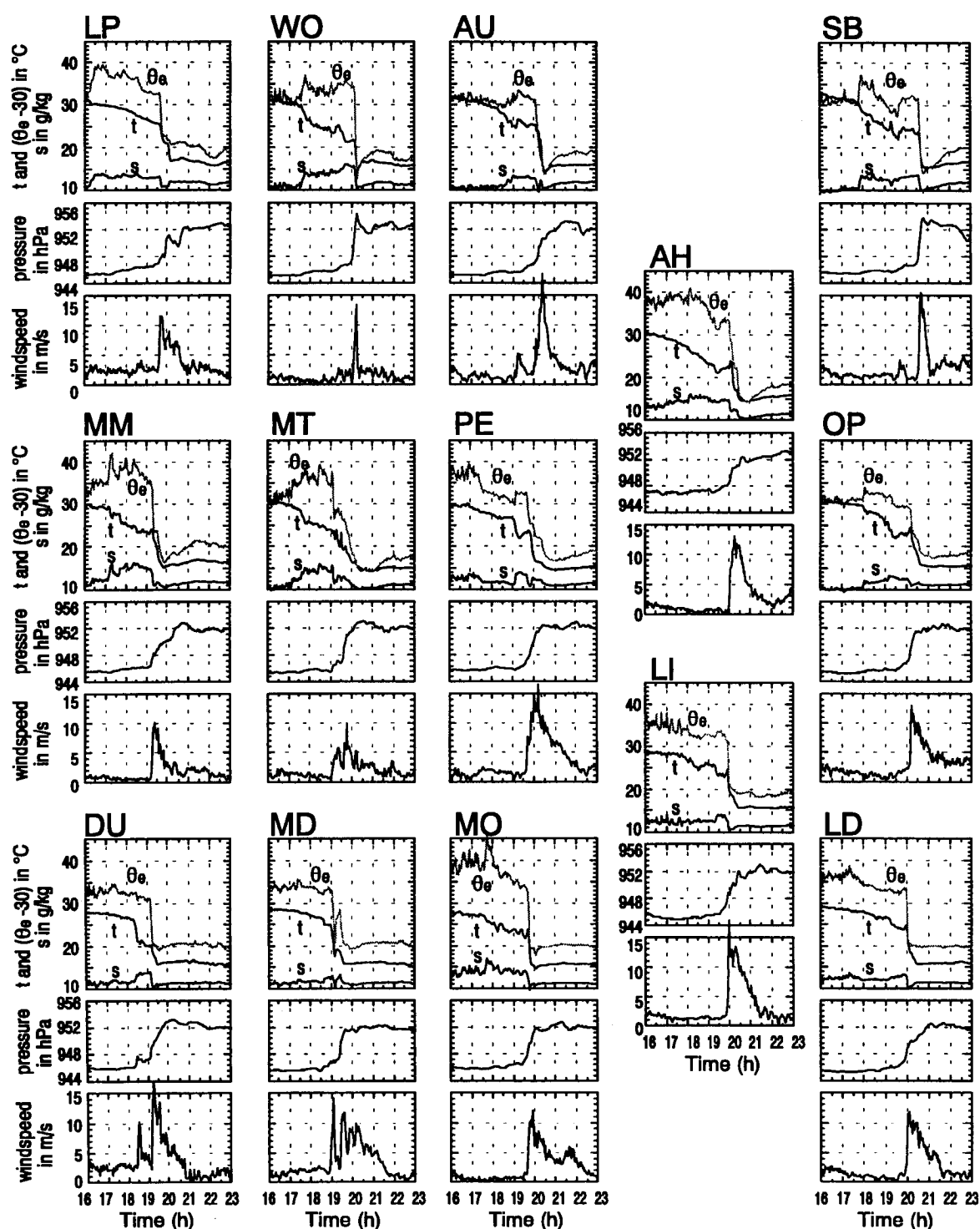
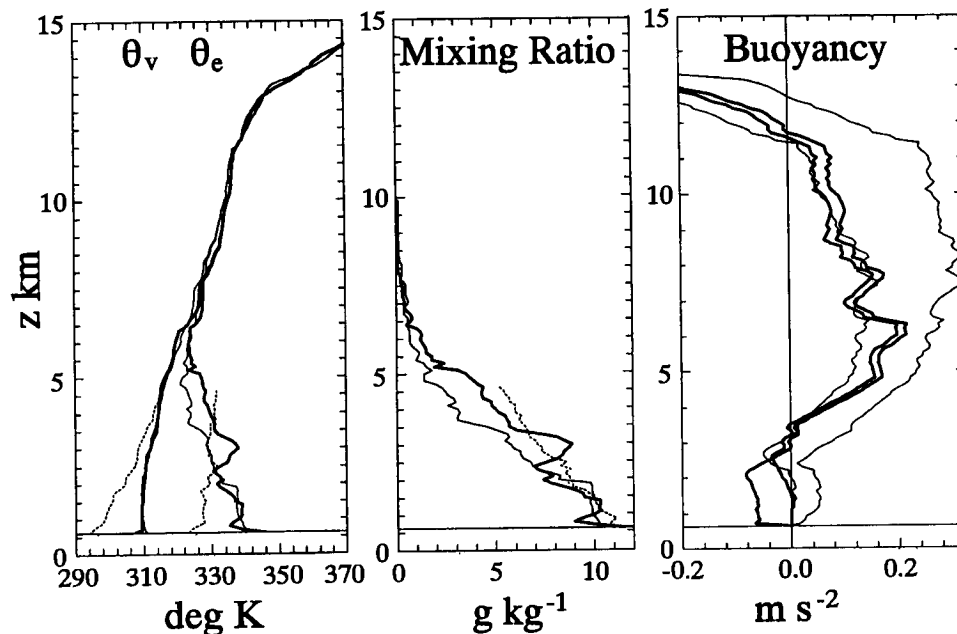


Figure 10: Overview of the mesonet data in the region between the River Danube and the northern edge of the Alps around the time of passage of the disturbance, between 1600 UTC and 2300 UTC on 21 July 1992. Locations of the stations are indicated in Figure 5 and 13. Shown at each station in order from top to bottom are time series of equivalent potential temperature, temperature, specific humidity, pressure reduced to the station height of Oberpfaffenhofen (581 m), and the wind speed. The data are based on two-minute mean values.



**Figure 11:** Vertical profiles of virtual potential temperature, pseudo-equivalent-potential temperature, mixing ratio, and the profile of buoyancy derived from the Penzing radiosonde sounding at 1400 (thin lines), 1800 UTC (thick lines), and 2100 UTC (dashed lines) on 21 July 1992. The buoyancy profiles relate to air parcels lifted from the surface and from a heights of 500 m above the surface, assuming pseudoadiabatic ascent.

By 1900 UTC, thunderstorms had developed all along the low pressure trough (see composite in Figure 7). Between the stationary convergence line 2b' and the approaching convergence line (Line 2c) there was a weak high pressure ridge with relatively weak gradients in the entire region between München and Lake of Constance. There was a region of low  $\theta_e$  underneath the cloud band of Line 2a with a minimum in the south. The time series of the corresponding mesonet sites Mattsies (MT) shortly after 1900 UTC and Wollbach (WO) at 2000 UTC show that the low values in  $\theta_e$  were a result of the air becoming cooler as well as drier. In the south, for example at Marktoberdorf (MD),  $\theta_e$  decreased rapidly by about 10 K within a quarter of an hour. The fall in temperature was presumably caused by a combination of the evaporative of precipitation below the developing thunderstorms and the descent of low  $\theta_e$  air in downdraughts from mid-tropospheric levels. The southwestern most mesonet site Durach (DU) was the first to be reached by Line 2c. Between 1800 UTC and 1900 UTC,  $q_e$  remained unchanged, while the temperature dropped by about 7 K and the moisture content of the air increased by about 4 g kg<sup>-1</sup>. This is indicative of precipitation cooled air related to thunderstorms along the Line 2b', but not of downdraught air. Line 2c, itself, passed the mesonet sites from

the southwest at about 1910 UTC (see Durach, DU) to the northeast at about 2045 UTC (see Sattelberg, SB). Its passage was accompanied with more or less abrupt changes in all variables, as can be seen on Figure 10.

By 1930 UTC, as shown on the composite of Figure 8, convergence line 2c had moved further eastwards and had caught up with the stationary convergence line (2b'). Thereafter the combined system moved eastwards.

At 2000 UTC an extensive system of the combined Lines 2 had formed with a large pressure gradient across its leading edge near the Alps of around 10 hPa in 50 km (see Figure 9). The system, characterized distinctly by this large pressure gradient moved rapidly eastwards, the average speed from 1900 UTC to 2000 UTC being 23 m s<sup>-1</sup>. The northern part of Line 2c moved at a much lower speed (12 m s<sup>-1</sup>). The mountains blocked the northerly flow behind the system of Lines 2, leading to an eastward acceleration in the vicinity of the mountains. This phenomena was named "orographic jet" by Egger and Haderlein (1987). The resulting bulk-like shape of the squall line resembles that of the well-documented "papal front" on 3 May 1987 (Volkert et al., 1991).



By 2000 UTC Line 3 had not yet reached southern Germany.

Figures 11 and 12 show the measurements by the Penzing radiosondes at 1400 UTC, 1800 UTC and 2100 UTC. The profile of the virtual potential temperature ( $\theta_v$ ) at 1400 UTC shows a mixed layer about 1.7 km deep that was markedly superadiabatic at low levels, indicative of vigorous convective mixing. By 1800 UTC, the mixed layer had deepened slightly, but a shallow radiation inversion had begun to develop in the lowest 100 m, indicating that convective mixing had ceased. The tropopause was located at a height a little above 11 km. The  $\theta_e$  profiles have a minimum at a height of about 5 km, an indication of potential instability. Of interest is a significant increase in moisture ( $2\text{--}3 \text{ g kg}^{-1}$ ) in the layer between 2 and 5 km over the four-hour period between the two soundings. This was presumably a consequence of advection by the westerly flow at these levels. After the passage of the squall line (2100 UTC sounding) the temperature is declined and the humidity increased.

Shown also in Figure 11 are profiles of the buoyancy force,  $B(z, z_L)$ , of air parcels lifted pseudo-adiabatically from a height  $z_L$  to a height  $z$ , as deduced from the foregoing radiosonde soundings. Calculations are shown for six values of  $z_L$  ranging from the surface ( $z = 0 \text{ m}$ ) to 500 m in steps of 100 m.

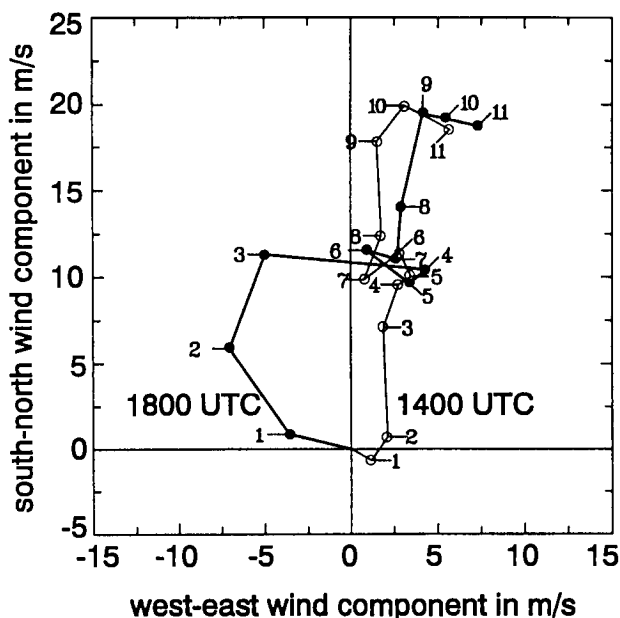


Figure 12: Hodographs for the Penzing radiosonde sounding at 1400 (thin line) and at 1800 UTC (thick line) on 21 July 1992. The labels indicate the height above mean sea-level.

The convective inhibition (CIN) is defined as the vertical integral of the buoyancy force over the intervals where it is negative between  $z_L$  and the level of free convection,  $z_{LFC}$ , the highest level at which  $B(z, z_L)$  becomes positive. The buoyancy of an air parcel lifted from the surface was appreciably larger at 1400 UTC than for one lifted from 100 m or more above the surface and hence  $\text{CAPE}(0)$  was appreciably larger than  $\text{CAPE}(z_L)$  for  $z_L \geq 100 \text{ m}$ . Table 1 lists the values of  $\text{CAPE}(z_L)$  and  $\text{CIN}(z_L)$  for  $z_L = 0 \text{ m}$  to  $500 \text{ m}$  in  $100 \text{ m}$  intervals for the two soundings and for the one at 1000 UTC. The table shows also the average value  $\text{ACAPE}$ , obtained by averaging the values of  $\text{CAPE}(z_L)$  over the five values of  $z_L \geq 100 \text{ m}$ . The existence of an appreciable minimum value of CIN for the six heights  $z_L$  indicates that lifting would have been necessary to initiate or maintain deep convection at the location of the sounding. This is in accordance with our hypothesis specified in Section 2. A value of  $\text{CIN} = 34 \text{ J kg}^{-1}$ , the minimum value at Penzing two hours before the passage of the squall line, would have required an air parcel of unit mass to have a vertical kinetic energy in excess of CIN to overcome the stability afforded by the negative area. This corresponds to a vertical velocity of about  $8 \text{ m s}^{-1}$ . Convective eddies with such high values are unlikely to have been present near the top of the mixed layer at that time, especially since dry convection would have been subsiding at that stage. Other values of CIN listed in Table 1 are mostly well in excess of  $34 \text{ J kg}^{-1}$ .

Besides CAPE and CIN we define a nondimensional number, the bulk Richardson number ( $Ri$ ), which combines the effects of CAPE and the vertical wind shear controlling storm structure and evolution. The bulk Richardson number is the ratio of the total energy available due to buoyancy to the total energy available from vertical shear (Bluestein and Jain, 1985). With a windshear of  $10.3 \text{ m s}^{-1}$  between a height of  $0.5 \text{ km}$  and  $6 \text{ km}$  and a  $\text{CAPE}(0)$  of  $973 \text{ J Kg}^{-1}$  at 1800 UTC we observe a value of  $Ri = 18.3$ . Following Weisman and Klemp (1982), low values of  $Ri$  (roughly between 5 and 35) favour the development of supercells. Further values of  $Ri$  for the different times are shown in Table 1.

In both soundings (Figure 12) the winds above about  $3 \text{ km}$  were westerly through a deep layer, with a maximum just below the tropopause. At 1400 UTC the wind direction below  $2 \text{ km}$  was directed mainly from west-northwest. At 1800 UTC the wind direction veered with height in the lowest  $3 \text{ km}$ , from a light northerly at the surface to a southeasterly above.

**Table 1:** Values of  $CAPE(z_L)$ ,  $CIN(z_L)$  and  $Ri(0)$  at Penzing on 21 July 1992 at the times indicated for values of  $z_L$  between the surface and 500 m in steps of 100 m, together with the average value of CAPE at the five levels from 100 m to 500 m, designated ACAPE.

$z_L$	1000 UTC		1400 UTC		1800 UTC	
	$CAPE(z_L)$	$CIN(z_L)$	$CAPE(z_L)$	$CIN(z_L)$	$CAPE(z_L)$	$CIN(z_L)$
0 m	1730	0	2294	0	973	123
100 m	797	45	1001	12	443	59
200 m	497	76	1004	15	319	81
300 m	499	73	903	20	466	59
400 m	576	68	704	31	750	34
500 m	593	67	675	37	734	37
ACAPE	592	65	857	23	542	54
$Ri(0)$	26.2		25.1		18.3	

These kinds of wind and potential-temperature profiles are typical of long-lived mesoscale convective systems observed in southern Germany (Höller et al., 1994). No wind data were available for the 2100 UTC sounding.

## 5 Meso- $\gamma$ -Scale Features

As might be expected, the line structures that are a feature of the meso- $\beta$ -scale analyses reveal considerable structure when viewed on the meso- $\gamma$ -scale. This is evident from the radar reflectivity patterns over southern Germany shown in Figure 13. The four panels in this figure span the period from 1927 UTC to 2005 UTC and indicate the positions of the surface gust fronts and the positions of the cloud/convergence lines in the meso- $\beta$ -scale analyses. The most prominent feature is the almost stationary line, Line 2b', which is marked also in Figure 8. The sequence of figures shows also the approach and merger of the convergence line (denoted Line 2c in Section 4 with the stationary Allgäu line (Line 2b')). At the leading edge of these two convergence lines, individual cells, named A, B and D, had formed. At 1937 UTC (Figure 13b) these cells were moving at speeds of  $8 \text{ m s}^{-1}$ ,  $30 \text{ m s}^{-1}$  and  $11 \text{ m s}^{-1}$ , respectively. Figures 13a to 13d show the high temporal variance in the intensity of the cells. This indicates the short lifetime of individual cells within a multi-cell convective system.

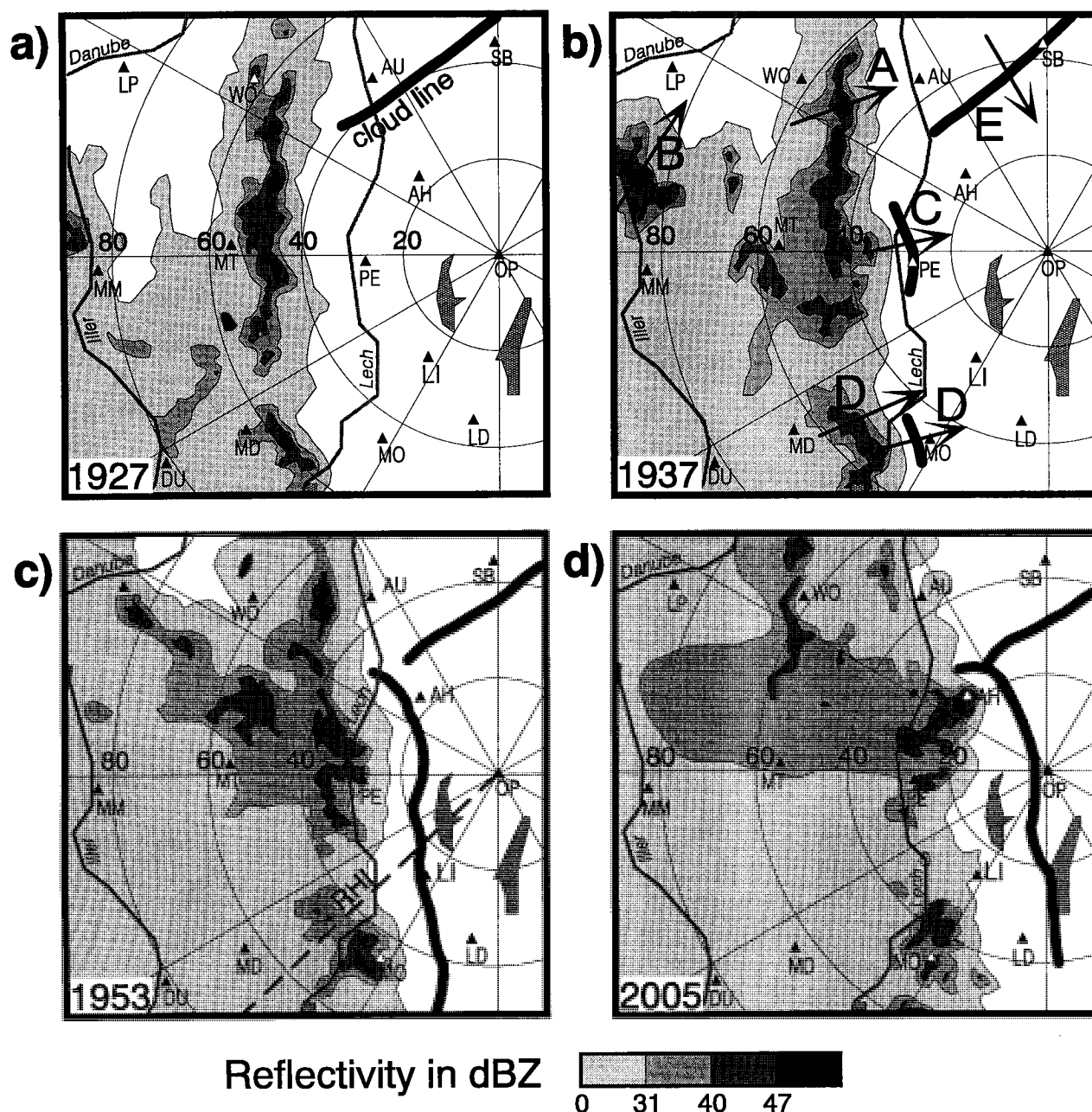
The cloud line marked E in Figure 13 is associated with the southern end of the former line 2a, and has reflectivity values between 10 dBZ and 0 dBZ, a typical range of values for nonprecipitating clouds. The thunderstorms along the convergence lines are

sources of low-level cold air arising from the evaporation of precipitation. Gust fronts C, D and E were moving at speeds  $15 \text{ m s}^{-1}$ ,  $16 \text{ m s}^{-1}$  and  $8 \text{ m s}^{-1}$ , respectively. These differ from the cell speeds as well as from the surface wind speeds immediately following the gust fronts. In the mesonet composite of Figure 10, the passage of gust fronts E and C is seen to have been accompanied by a local kink in the  $\theta_e$ -traces at Augsburg (AU), Altheim (AH) and Penzing (PE). When gust front D passed the Lichtenau (LI) site at 1953 UTC, wind speeds of more than  $18 \text{ m s}^{-1}$  were recorded at the surface (see Figure 10) and up to  $24 \text{ m s}^{-1}$  at a height of 70 m above ground (Finke and Hauf, 1994).

The flow pattern in a vertical Doppler RHI<sup>4</sup>-scan towards the southwest (along the dashed line in Figure 13) displays the cold-air outflow and gust front at the surface at 1950 UTC produced by the evaporation of precipitation beneath cell D of Line 2b' (see Figure 14). Here, wind speeds behind the gust front exceeded  $25 \text{ m s}^{-1}$  towards the radar. There were high Doppler velocities towards the radar within the cell and on its rear side also, and two regions of horizontal convergence. One of them is located at a distance of about 43 km, the inflow being positioned above the gust front; the resulting updraught diverges into an anvil beneath the tropopause. A secondary convergence region is located at a range of about 56 km. Here hail was indicated by the polarimetric radar data (Hagen and Höller, 1994). This structure of a rear inflow is typical for squall lines (Meischner et al., 1991).

Figure 15 shows a detailed view of the reflectivity (a) and the Doppler velocity (b) at 1946 UTC during the

<sup>4</sup> Range Height Indicator



merging of the lines 2c and 2b'. Besides the precipitation area the gust fronts C and D are also visible ahead of the squall line. The propagation speed of the system ( $11 \text{ m s}^{-1}$ ) has to be subtracted from the measured Doppler velocity in order to consider the relative motion within the storm cells. At least four major storm cells (A to D) are found in the reflectivity im-

age. Cell A belongs to line 2b'. Only weak Doppler velocities are observed in this cell. This agrees well with the measurements of the surface network showing no or only weak diffluent flow along line 2b'. Cell B is attached to line 2c, cell C at the merging point and cell D along the already merged squall line. High Doppler velocities towards the radar are observed

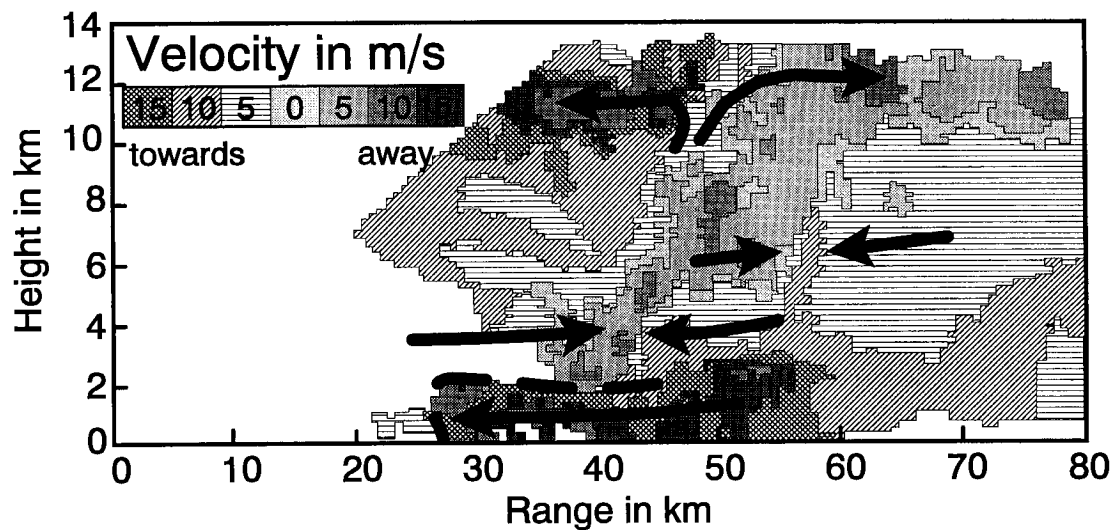


**Figure 14:** Range Height Indicator (RHI) at 1950 UTC, showing Doppler velocity. The arrows indicate the relative flow, the dashed line marks the gust front flow. The Doppler velocity was aliased at  $16.35 \text{ m s}^{-1}$ . Note, an observed speed of  $10 \text{ m s}^{-1}$  away from the radar has to be interpreted as  $22 \text{ m s}^{-1}$  towards the radar. (Taken from Hagen and Höller, 1994)

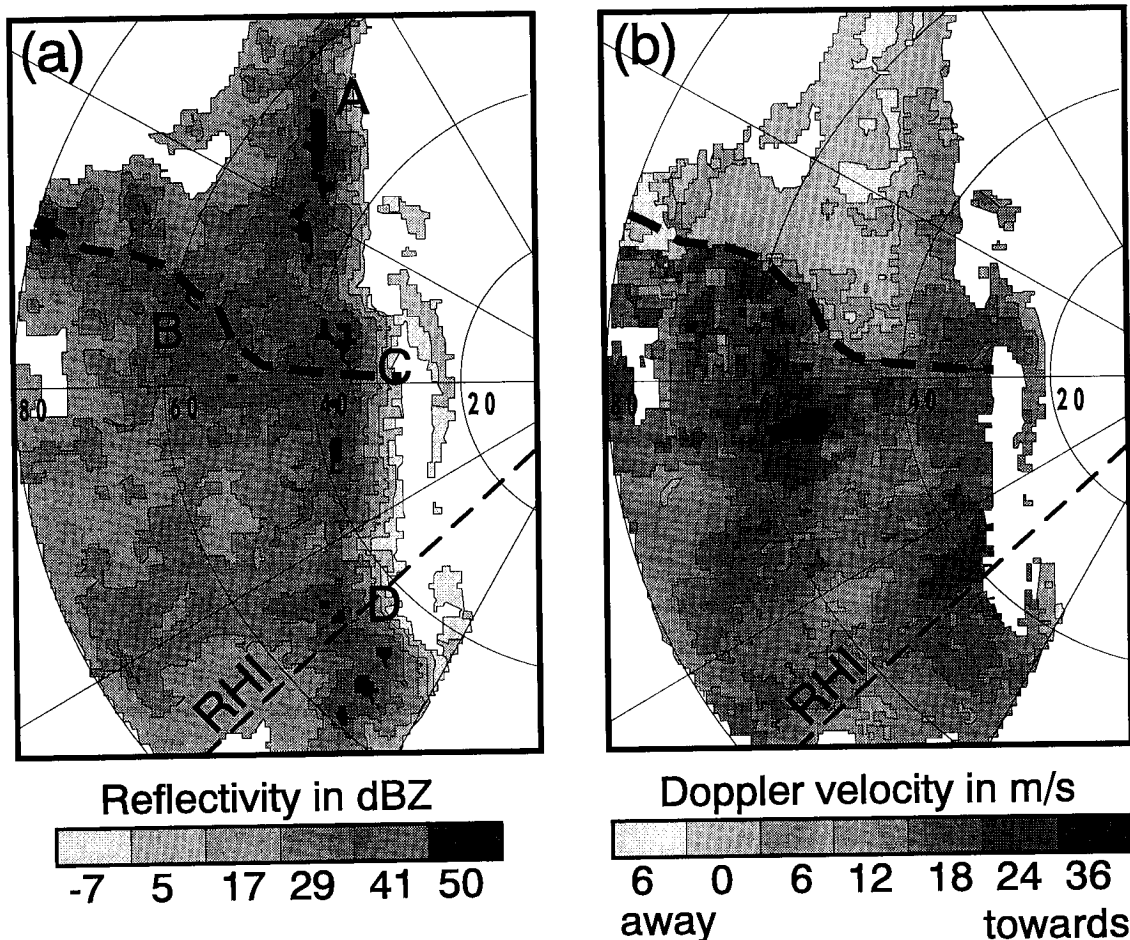


**Figure 15:** Plan Position Indicator (PPI) at 1946 UTC, showing Reflectivity (a) and Doppler velocity (b). The dashed line named RHI shows the orientation of the RHI of Figure 14. The bold dashed line separates the squall line from line 2b'.



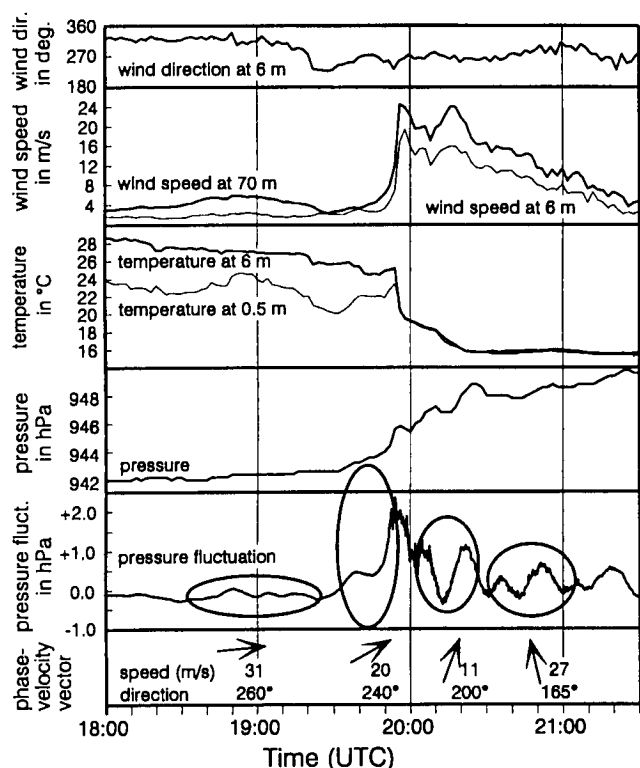


**Figure 16:** Time series of wind, temperature pressure and pressure fluctuations at Lichtenau. Pressure measurements are at the surface. Phase-velocity vectors are determined from the indicated intervals.

within these three cells and on their rear side. This flow structure is maintained by latent heat release in the stratiform precipitation, and is a typical characteristic of squall lines. The shear of the Doppler velocity allows to distinguish the squall line (2c) from the preceding line 2b' along the dashed line in Figure 15b.

By 2005 UTC several new cells had formed at a distance of 25 km northwest of the radar (see Figure 13d). These were presumably initiated by convergence produced at the intersection of Lines 2b' and 2c.

As noted above, the gust front D passed the Lichtenau (LI) at about 1953 UTC (see Figure 13c) where it was recorded by a network of four ultra-sensitive microbarographs (Finke and Hauf, 1994). From the times of passage at the four instruments, the propagation speed and direction of the gust front could be determined. Figure 16 summarizes data from the Lichtenau site. It depicts time series of wind direction and wind speed at heights of 6 m and 70 m, temperatures at 0.5 m and 6 m, the surface-pressure fluctuations, absolute pressure, and the translation velocity. While the maximum pressure fluctuation at 1953 UTC marks gust front D, there was a bow wave which preceded the gust front by about 15 min. At the time of the bow-wave passage, a radiative surface

inversion of about 100 m had already become established (see Beyrich et al., 1994; and Lösslein, 1994). The temperature trace shows that the air at a height of 6 m became colder following the bow-wave passage, whereas mixing down of potentially-warm air resulted in a temperature increase at the surface of about 2 K. The mixing was recorded also by the sodar at the Lichtenau, which measures the amount of the backscatter signal to small-scale temperature fluctuations during mixing (see Beyrich et al., 1994). The passage of the gust front was accompanied by strong winds and advected cold air into the mesonet region (see Figure 10). The interface between this cold air and the warmer air above provided a possible waveguide for the gravity waves that were observed during the two hours following the passage of the gust front at the Lichtenau.

At about 1840 UTC, well ahead of the gust front and its bow wave, there was a set of waves (see left arrow on Figure 16). Their large propagation speed of  $31 \text{ m s}^{-1}$  suggests that they were radiated away from the Line 2b'. Examination of the high-pass filtered pressure traces of the four southernmost mesonet sites leads one to infer that the generation occurred in a thunderstorm cell within the Allgäu line close to Durach (see Figure 10; and Luckner and Smith, 1994).

## 6 Conclusions

The sequence of events surrounding the initiation and development of the storm on 21 July 1992 fits well with the hypothesis that was formulated prior to the CLEOPATRA experiment and its sub-project "mission squall line" (Meischner et al., 1993). In particular, the storm developed in a southwesterly airstream on a summer's day, when the low level advection of warm and moist, potentially unstable air was large to the north of the Alps. Large-scale lifting was necessary to destabilize the air mass. This lifting was forced in the region ahead of the trough which was approaching from the west.

The large-scale southwesterly airflow was deflected at low levels around the Alps while at high levels it crossed the mountains. This created the observed situation ahead of the squall line (Line 2c) with low pressure along the northern rim of the Alps, low-level convergence lines (1, 2a, 2b, and 2b'), and a wind vector veering with height. The resulting wind profile supported the longevity of the mesoscale convective system. The mesoscale features of this storm agreed well with criteria from other observations of squall

lines, e.g. the values for CAPE and the bulk Richardson number.

An interesting feature of the squall-line development was observed in the Allgäu region. The eastward moving squall line (Line 2c) caught up with a pre-existing, almost stationary line (Line 2b') of thunderstorms. After merging the squall line intensified and accelerated considerably. The process of merging of the two lines could be observed in detail since it happened in the range of DLR's Doppler radar and in the area in which the temporary mesonet was installed. A similar merging of a moving line with a pre-existing stationary line of thunderstorms took place some hours earlier in Switzerland (Schiesser et al., 1994).

Owing to the additional meteorological measuring equipment in the course of the CLEOPATRA experiment, the squall line of 21 July 1992 is, so far, the best documented case of its kind in southern Germany. We think that this day provides an ideal validation data base for subsequent numerical studies and improvements of high resolution weather prediction models. Besides being a challenge to forecast models anyway, the extremely severe weather happened on a spatial scale that is too small as to be captured by the routine meteorological network. The availability of complementary measurements such as the mesonet, additional radiosoundings, and the complete coverage by a scientific radar, are therefore seen as a unique chance for the aforementioned purpose.

## Acknowledgements

We thank Dr. H. Schroers for providing the analyzed mesonet data, the Schweizer Meteorologische Anstalt (SMA) and the Deutscher Wetterdienst (DWD) for the radar data and M. Jaeneke (DWD) for supplying us with other case studies on that same event. We acknowledge financial support for the project from the German Research Council (Deutsche Forschungsgemeinschaft).

## References

- Berliner Wetterkarte*; issued by the Freie Universität Berlin.
- Beyrich F.; Kalass, D. and Weisensee, U.; 1994: Boundary-layer structure and wind field at the DLR-site Lichtenau as observed with Doppler-Sodar. The squall line of 21 July 1992 in Switzerland and southern Germany - a documentation. DLR Forschungsbericht 94-18, pp163, obtainable from DLR, Linder Höhe, D-51147 Köln, Germany.
- Bluestein, H.B. and Jain, M.H.; 1985: Formation of mesoscale lines of precipitation: severe squall lines in Oklahoma during the spring. *J. Atmos. Sci.* **42**, 1711–1732.
- Browning, K.A. and Ludlam, F.H.; 1962: Airflow in convective storms. *Q. J. R. Meteorol. Soc.* **88**, 117–135.
- Brugge, R. and Moncrieff, M.W.; 1992: Multicell stage of the München storm of 12 July 1984: a numerical study. *Tellus* **44A**, 339–355.
- Court, A. and Griffiths, J.F.; 1985: Thunderstorm climatology. In: Kessler (ed); *Thunderstorm morphology and dynamics*, Univ. of Oklahoma Press, Norman, Okl. USA, 411 pp.
- Emanuel, K.A.; 1994: *Atmospheric convection*. Oxford Univ. Press, 580 pp.
- Egger, J. and Haderlein, K.; 1987: Fronts near orography in a one-layer model. *J. Met. Soc. Jap.* **65**, 757–766.
- Finke, U. and Hauf, T.; 1994: High-frequency surface-pressure measurements in Lichtenau. The squall line of 21 July 1992 in Switzerland and southern Germany - a documentation. DLR Forschungsbericht 94-18, pp153, obtainable from DLR, Linder Höhe, D-51147 Köln, Germany.
- Finke, U. and Hauf, T. (eds.); 1997: The severe convective storms in central Europe on July 21, 1992 - A research dataset. DLR-Mitteilung 97-02, (CD-ROM), obtainable from DLR, Linder Höhe, D-51147 Köln, Germany.
- Garrett, J.G.; Physick, W.L.; Smith, R.K. and Troup, A.J.; 1985: The Australian summertime cool change. Part II: Mesoscale aspects. *Mon. Wea. Rev.* **113**, 202–223.
- Haase-Straub, S.P.; Heimann, D.; Hauf, T.; Smith, R.K. (eds.); 1994: The squall line of 21 July 1992 in Switzerland and southern Germany - a documentation. DLR Forschungsbericht 94-18, 226 pp., obtainable from DLR, Linder Höhe, D-51147 Köln, Germany.
- Hagen, M. and Heimann, D.; 1994: Detailed analyses of the squall line over Southern Germany. The squall line of 21 July 1992 in Switzerland and southern Germany - a documentation. DLR Forschungsbericht 94-18, pp67, obtainable from DLR, Linder Höhe, D-51147 Köln, Germany.
- Hagen, M. and Höller, H.; 1994: Small-scale Doppler and polarimetric radar observations. The squall line of 21 July 1992 in Switzerland and southern Germany - a documentation. DLR Forschungsbericht 94-18, pp147, obtainable from DLR, Linder Höhe, D-51147 Köln, Germany.
- Heimann, D. and Kurz, M.; 1985: The München hailstorm of July 12, 1984: A discussion of the synoptic situation. *Beitr. Phys. Atmosph.* **58**, 528–544.
- Höller, H.; 1994: Mesoscale organization and hailfall characteristics of deep convection in southern Germany. *Beitr. Phys. Atmosph.* **67**, 219–234.
- Höller, H. and Reinhardt, M.; 1986: The München hailstorm of 12 July 1984: Convective development and preliminary hailstorm analysis. *Beitr. Phys. Atmosph.* **59**, 1–2.
- Höller, H.; Bringi, V. N.; Hubbert, J.; Hagen M. and Meischner, P.F.; 1994: Life cycle and precipitation formation in a hybrid-type hailstorm revealed by polari-

- metric and Doppler radar measurements. *J. Atmos. Sci.* **51**, 2500.
- Houze, R.A.; 1993: Cloud dynamics. Intern. Geophys. Series, Academic Press, New York, **53**, 573 pp.
- Houze, R.A. and Hobbs, P.V.; 1982: Organization and structure of precipitation cloud systems. *Adv. in Geoph.* **24**, 225–315.
- Houze, R.A.; Smull, B.F. and Dodge, P.; 1990: Mesoscale organization of springtime rainstorms in Oklahoma. *Mon. Wea. Rev.* **118**, 613–654.
- Huntriesser, H.; 1995: Zur Bildung, Verteilung und Vorhersage von Gewittern in der Schweiz. Doctoral dissertation, ETH Zürich, pp 246.
- Keers, J.F. and Westcott, P.; 1976: The Hamstead storm 14 August 1975. *Weather* **31**, 2–10.
- Kessler, E.; 1985: Thunderstorm morphology and dynamics. Univ. of Oklahoma Press, Norman, Okl., USA, 411 pp.
- Luckner, R. and Smith, R.K.; 1994: Objective analyses of surface network and aircraft data. The squall line of 21 July 1992 in Switzerland and southern Germany - a documentation. DLR Forschungsbericht 94-18, pp95, obtainable from DLR, Linder Höhe, D-51147 Köln, Germany.
- Lösslein, H.; 1994: The squall line passage at the meteorological tower in Garching. The squall line of 21 July 1992 in Switzerland and southern Germany - a documentation. DLR Forschungsbericht 94-18, pp133, obtainable from DLR, Linder Höhe, D-51147 Köln, Germany.
- Meischner, P.F.; Bringi, V.N.; Heimann, D. and Höller, H.; 1991: A squall line in southern Germany: kinematics and precipitation formation as deduced by advanced polarimetric and Doppler radar measurements. *Mon. Wea. Rev.* **119**, 678–701.
- Meischner, P.F.; Hagen, M.; Hauf, T.; Heimann, D.; Höller, H.; Schumann, U.; Jaeschke, W.; Mauser, W. and Pruppacher, H.R.; 1993: The field project CLEOPATRA, May–July 1992 in Southern Germany. *Bull. Amer. Met. Soc.* **74**, 401–412.
- Miller, M.J.; 1978: The Hampstead storm: A numerical simulation of a quasi-stationary cumulonimbus system. *Q. J. R. Meteorol. Soc.* **1040**, 413–427.
- Pelz, J.; 1984: Die geographische Verteilung der Tage mit Gewitter in Mitteleuropa. Beilage zur Berliner Wetterkarte 48/84 SO 12/84, 32 pp.
- Prenosil, T.; Thiel, D. and Kraus, H.; 1995: Frontogenesis and cross frontal circulation in a strong summertime cold front. *Meteorol. Atmos. Phys.* **56**, 181–196.
- Schiesser, H.H.; Houze Jr., R.A. and Huntrieser, H.; 1995: The mesoscale structure of severe precipitation systems in Switzerland. *Mon. Wea. Rev.* **123**, 2070–2097.
- Schroth, A.C.; Chandra, M.S. and Meischner, P.F.; 1988: A C-band coherent polarimetric radar for propagation and cloud physics research. *J. Atmos. Oceanic. Technol.* **5**, 803–822.
- Volkert, H.; Weikmann, L. and Tafferger, A.; 1991: The Pappal Front of 3 May 1987: A remarkable example of frontogenesis near the Alps. *Q. J. R. Meteorol. Soc.* **117**, 125–150.
- Weisman, M.L. and Klemp, J.B.; 1982: The dependence of numerically simulated convective storms on vertical wind shear and buoyancy. *Mon. Wea. Rev.* **110**, 504–520.
- Wyss and Emanuel, K.A.; 1988: Prestorm environment of midlatitude prefrontal squall lines. *Mon. Wea. Rev.* **116**, 790–794.